Journal of Mathematical Modeling
Vol. , No. , 2026, pp. -. Research Article

JMM

A computational framework for fractional integro-differential equations involving mixed integral terms

Siba Prasad Mohapatra[†*], **Anasuya Nath**[‡]

[†]*Department of Mathematics, Konark Institute of Science and Technology, India*
[‡] *Department of Mathematics, Utkal University, India*

Email(s): spmohapatra71@gmail.com, anasuya_nath@yahoo.com

Abstract. This paper proposes an efficient difference scheme for addressing Volterra integro-differential equations of fractional order with a mixed integral term. The fractional operator is taken in the Caputo sense of order $\sigma \in (0,1)$. We start by establishing sufficient conditions for the existence of a unique solution. The differential operator is discretized using the $L1$ method on a uniform grid, and composite trapezoidal formula is applied to approximate the mixed integral. A comprehensive convergence analysis is carried out under appropriate regularity conditions on the initial data. The findings show that the derived scheme achieves the convergence rate of $(2-\sigma)$. Numerical experiments are conducted to substantiate the theoretical conclusions and illustrate the effectiveness of the scheme.

Keywords: Caputo derivative, fractional integro-differential equation, mixed integral, $L1$ technique, trapezoidal formula, error estimation
AMS Subject Classification 2010: 26A33, 35R09, 45D05, 65R20

1 Introduction

Fractional calculus is an extension of classical calculus that broadens the concepts of derivatives and integrals to encompass non-integer orders. Nowadays, it has garnered significant interest due to its wide application in various disciplines, including physics, engineering, finance, biology, etc. For further details, refer to [2,6,7,16,18] and the related references for more information. In this instance, equations involving derivatives and integrals of non-integer order are referred to as fractional order integro-differential equations (FIDEs). Because the differentiation and integration operations can be of any real or complex order, these equations generalize classical integro-differential equations. When modeling systems with memory effects, hereditary characteristics, or processes exhibiting anomalous diffusion-where a

*Corresponding author
Received: 03 February 2026/ Revised: 11 May 2026/ Accepted: 12 May 2026
DOI: 10.22124/jmm.2026.32894.2993

system's future state is dependent on its complete history rather than just its current state-FIDEs are especially helpful. Applications for fractional order integro differential equations (FOIDEs) can be found in a variety of domains, including biological systems, signal processing, control theory, and viscoelasticity. They are used, for instance, in control theory to create controllers for systems with long-range temporal dependencies. They simulate phenomena such as anomalous diffusion in complex media in physics. As a result, fractional integro-differential equation solutions have advanced and are now a crucial area of applied mathematics.

The present work considers the following integro-differential equation of arbitrary order involving a mixed integral:

$$\begin{cases} \mathscr{D}_{x_1}^{\sigma} Z(x_1,x_2) + A(x_1,x_2)Z(x_1,x_2) + \lambda \int_0^{x_2}\int_0^{x_1} \mathscr{K}(x_1,x_2,r,s)Z(r,s)\,dr\,ds = g(x_1,x_2), \\ \text{for} \quad (x_1,x_2) \in (0,1]\times[0,1], \\ Z(0,x_2) = \phi(x_2) \quad \text{for} \quad x_2 \in [0,1], \end{cases} \tag{1}$$

where $\lambda \in \mathbb{R}$. Denote $\Omega := [0,1]\times[0,1]$. Assume that the coefficient $A : \Omega \to \mathbb{R}$ and the kernel function $\mathscr{K}(>0) : \Omega \times \Omega \to \mathbb{R}$ are sufficiently smooth. $\mathscr{D}_{x_1}^{\sigma}$ denotes the fractional differential operator.

It is extremely challenging to obtain exact solutions of fractional-order integral and integro-differential equations involving mixed integrals. As a result, a number of approximation-based analytical and numerical methods have attracted a lot of interest lately. Rahimi et al. [15] carried out a convergence analysis and suggested the Tau method to approximate the Fredholm-type integral equation with mixed integrals. A similar numerical technique based on Legendre orthogonal polynomials was developed in [17]. Nemati et al. [12] introduced operational matrices using shifted Legendre polynomials to approximate nonlinear 2D Volterra integral equations. In [11], Mojahedfar and Tari employed a 2D Legendre wavelet technique to investigate FIDEs involving mixed integrals. A computational method utilizing Mott polynomials combined with a 2D Legendre–Gauss quadrature formula was presented in [4] to approximate fractal-fractional Fredholm–Volterra IDEs. Ahsan et al. [1] applied the optimal homotopy asymptotic technique for approximating two-dimensional Volterra integro-differential equations of fractional order. Recently, Panda *et al.* [13] developed and tested two difference schemes based on the L1 technique to compute the numerical solution of a Volterra-type FIDE with a weakly singular kernel. Related numerical studies on time-fractional dynamical systems and some other models can be found in [3, 9, 10].

Motivated by the aforementioned research, we examine several features of the numerical approximation of FIDEs involving mixed integrals. However, the majority of the techniques referenced in the preceding literature are either semi-analytical or spectral/collocation methods, each possessing inherent constraints. At the same time, some work has been done to use the finite difference method to approximate the solutions of FIDEs. The main advantages of this difference method are its relative ease of use, clarity, and capacity to produce good results even with a small mesh size. Additionally, a detailed presentation of the convergence and stability studies of finite difference methods is provided. The primary goal of this study is to create an efficient finite difference method that approximates equation (1) by using the trapezoidal formula for the mixed integral term and $L1$ technique for discretizing the differential operator. Under appropriate smoothness assumptions on the initial data, it is demonstrated that the suggested scheme achieves a convergence rate of order $(2-\sigma)$. Finally, to confirm the theoretical results and effectiveness of the applied technique, a number of tables and graphs are presented along with numerical experiments. The primary advantages of this finite difference approach are its simplicity, ease

of implementation, and ability to yield accurate solutions even with relatively coarse meshes. In addition, the convergence and stability properties of finite difference schemes are well established. Because the domain in our study is rectangular-and therefore geometrically regular-finite difference methods are particularly well suited for obtaining reliable results. Similar to the finite difference method, the only drawback of the proposed technique is its applicability to physical problems defined on a irregular geometry. This article is structured as follows: Section 2 presents the necessary background on fractional calculus and proves the existence and uniqueness of the solution. Section 3 describes the construction of the proposed numerical technique. Error analysis is discussed in Section 4. Section 5 provides numerical illustrations. Finally, Section 6 concludes the work.
Notations: In a given domain D, the notation $\mathscr{C}^k(D)$ denotes functions that are k-times continuously differentiable. In this manuscript, C represents a generic positive constant that remains independent of the mesh parameters. $\|\xi\|_\infty = \max_k |\xi(t_k)|$ stands for supremum norm.

2 Preliminaries

The definitions and properties outlined here are essential for this study. For additional information, we refer to [5, 14].

Definition 1. *Let $f(z) \in \mathscr{C}[a,b]$. The Riemann-Liouville integral of order $\nu \in \mathbb{R}^+$ of $f(z)$ is defined as follows:*

$$J_z^\nu f(z) = \frac{1}{\Gamma(\nu)} \int_a^z (z-s)^{\nu-1} f(s)\, ds.$$

Definition 2. *Let $n-1 < \nu \le n$, $n \in \mathbb{N}$. The Caputo derivative of order $\nu \in \mathbb{R}^+$ of $f(z) \in \mathscr{C}^n[a,b]$, is defined as follows:*

$$\mathscr{D}_z^\nu f(z) = \begin{cases} \dfrac{1}{\Gamma(n-\nu)} \displaystyle\int_a^z (z-s)^{n-\nu-1} f^{(n)}(s)\, ds & \text{if} \quad n-1 < \nu < n, \\ f^{(n)}(z) & \text{if} \quad \nu = n. \end{cases}$$

Definition 3. *The Mittag–Leffler function with two parameters $\alpha_1, \alpha_2 > 0$ is defined as follows:*

$$E_{\alpha_1,\alpha_2}(z) = \sum_{k=0}^{\infty} \frac{z^k}{\Gamma(\alpha_1 k + \alpha_2)}, \qquad z \in \mathbb{C}.$$

- Linearity: Let λ_1, λ_2, be positive constants, then

$$J_z^\nu \{\lambda_1 \varphi_1(z) \pm \lambda_2 \varphi_2(z)\} = \lambda_1 J_z^\nu \varphi_1(z) \pm \lambda_2 J_z^\nu \varphi_2(z),$$
$$\mathscr{D}_z^\nu \{\lambda_1 \varphi_1(z) \pm \lambda_2 \varphi_2(z)\} = \lambda_1 \mathscr{D}_z^\nu \varphi_1(z) \pm \lambda_2 \mathscr{D}_z^\nu \varphi_2(z).$$

- For $z \in [a,b]$, $m-1 < \nu < m$, we have

$$\mathscr{D}_z^\nu J_z^\nu \varphi(z) = \varphi(z) \quad \text{and} \quad J_z^\nu \mathscr{D}_z^\nu \varphi(z) = \varphi(z) - \sum_{k=0}^{n-1} \varphi^{(k)}(a^+) \frac{(z-a)^k}{k!}, \quad z > a.$$

Theorem 1. *Problem (1) has a unique solution in* Ω *if* $\dfrac{(\sigma+1)\zeta+\mu\eta}{\Gamma(2+\sigma)}<1.$

Proof. Applying $J^{\sigma}_{x_1}$ to (1), one has

$$Z(x_1,x_2)=\Psi(Z(x_1,x_2)) \quad \text{in } \Omega,$$

where

$$\Psi(Z(x_1,x_2))=\phi(x_2)+J^{\sigma}_{x_1}g(x_1,x_2)-J^{\sigma}_{x_1}\left[A(x_1,x_2)Z(x_1,x_2)\right]-\lambda J^{\sigma}_{x_1}\Big[\int_0^{x_2}\int_0^{x_1}\mathscr{K}(x_1,x_2,r,s)Z(r,s)\,dr\,ds\Big].$$

Let $Z_1(x_1,x_2)$ and $Z_2(x_1,x_2)$ be any two functions in the space $\mathscr{C}([0,1]\times[0,1],\mathbb{R})$. We have

$$\begin{aligned}\left\|\Psi(Z_1(x_1,x_2))-\Psi(Z_2(x_1,x_2))\right\| &\le \left\|J^{\sigma}_{x_1}\Big\{A(x_1,x_2)\big(Z_1(x_1,x_2)-Z_2(x_1,x_2)\big)\Big\}\right\|\\ &\quad+\lambda\left\|J^{\sigma}_{x_1}\Big\{\int_0^{x_2}\int_0^{x_1}\mathscr{K}(x_1,x_2,r,s)\big(Z_1(r,s)-Z_2(r,s)\big)\,dr\,ds\Big\}\right\|\\ &\le \frac{1}{\Gamma(\sigma)}\left\|\int_0^{x_1}\frac{|A(t,x_2)|\,|Z_1(t,x_2)-Z_2(t,x_2)|}{(x_1-t)^{1-\sigma}}\,dt\right\|\\ &\quad+\frac{\mu}{\Gamma(\sigma)}\left\|\int_0^{x_1}\Big\{\int_0^{x_2}\int_0^{t}|\mathscr{K}(t,x_2,r,s)|\,|Z_1(r,s)-Z_2(r,s)|\,dr\,ds\Big\}\frac{dt}{(x_1-t)^{1-\sigma}}\right\|.\end{aligned}$$

Since the functions $\mathscr{K}$ and A are both bounded, there exist constants $\eta>0$ and $\zeta>0$ such that $\left|\mathscr{K}(x_1,x_2,r,s)\right|\le\eta$ and $\left|A(x_1,x_2)\right|\le\zeta$. Therefore, we obtain

$$\begin{aligned}\left\|\Psi(Z_1(x_1,x_2))-\Psi(Z_2(x_1,x_2))\right\| &\le \frac{\zeta}{\Gamma(\sigma)}\left\|Z_1(x_1,x_2)-Z_2(x_1,x_2)\right\|\times\left|\int_0^{x_1}(x_1-t)^{\sigma-1}dt\right|\\ &\quad+\frac{\mu\eta}{\Gamma(\sigma)}\left\|Z_1(x_1,x_2)-Z_2(x_1,x_2)\right\|\times\left|\int_0^{x_1}(x_1-t)^{\sigma-1}\Big\{\int_0^{x_2}\int_0^{t}dr\,ds\Big\}dt\right|\\ &\le \frac{(\sigma+1)\zeta+\mu\eta}{\Gamma(2+\sigma)}\left\|Z_1(x_1,x_2)-Z_2(x_1,x_2)\right\|\\ &< \left\|Z_1(x_1,x_2)-Z_2(x_1,x_2)\right\|.\end{aligned}$$

Thus, Ψ satisfies the contraction property. Since $\big(\mathscr{C}(\Omega),\|\cdot\|\big)$ is a Banach space, the Banach fixed-point theorem guarantees that Ψ possesses a unique fixed point, which represents the solution of (1). □

3 Proposed scheme

Let N_{x_1} and N_{x_2} be positive integers. We introduce a uniform grid with mesh points $(x_1)_j=jh_{x_1}$ for $j=0,1,\ldots,N_{x_1}$, where the mesh size is $h_{x_1}=N_{x_1}^{-1}$, $(x_2)_i=ih_{x_2}$ for $i=0,1,\ldots,N_{x_2}$, and $h_{x_2}=N_{x_2}^{-1}$. Also Z^i_j denotes the numerical approximation to Z at the grid point $((x_1)_j,(x_2)_i)\in\Omega^{N_{x_2}}_{N_{x_1}}$. Caputo's fractional derivative $\mathscr{D}^{\sigma}_{x_1}Z((x_1)_j,(x_2)_i)$ at $((x_1)_j,(x_2)_i)$ is expressed as follows:

$$\mathscr{D}^{\sigma}_{x_1}Z((x_1)_j,(x_2)_i)=\frac{1}{\Gamma(1-\sigma)}\sum_{k=0}^{j-1}\int_{s=(x_1)_k}^{(x_1)_{k+1}}((x_1)_j-s)^{-\sigma}\frac{dZ}{ds}(s,(x_2)_i)ds. \tag{2}$$

The $L1$ approximation [8] of (2) is

$$\begin{aligned}\mathscr{D}^{\sigma}_{N_{x_1}} Z((x_1)_j,(x_2)_i) &= \frac{1}{\Gamma(1-\sigma)}\sum_{k=0}^{j-1}\frac{Z((x_1)_{k+1},(x_2)_i)-Z((x_1)_k,(x_2)_i)}{h_{x_1}}\int_{s=(x_1)_k}^{(x_1)_{k+1}}((x_1)_j-s)^{-\sigma}ds\\ &= \frac{h_{x_1}^{-\sigma}}{\Gamma(2-\sigma)}\sum_{k=0}^{j-1}\left[Z((x_1)_{k+1},(x_2)_i)-Z((x_1)_k,(x_2)_j)\right]d_{j-k},\end{aligned} \tag{3}$$

where $d_q = q^{1-\sigma}-(l-q)^{1-\sigma},\ \ q=1,2,\ldots,N_{x_1}$. Let $\varepsilon^i_j = \left(\mathscr{D}^{\sigma}_{x_1}-\mathscr{D}^{\sigma}_{N_{x_1}}\right)Z((x_1)_j,(x_2)_i)$ denotes the truncation error. Integral expression for $j=1,2,\ldots,N_{x_1}$ and $i=1,2,\ldots,N_{x_2}$ can be reformulated as follows:

$$\begin{aligned}I_{x_1,x_2}Z((x_1)_j,(x_2)_i) &= \int_0^{(x_2)_i}\int_0^{(x_1)_j}\mathscr{K}((x_1)_j,(x_2)_i,r,s)Z(r,s)\,drds\\ &= \sum_{p=0}^{i-1}\sum_{k=0}^{j-1}\int_{(x_2)_p}^{(x_2)_{p+1}}\int_{(x_1)_k}^{(x_1)_{k+1}}\mathscr{K}((x_1)_j,(x_2)_i,r,s)Z(r,s)\,drds.\end{aligned} \tag{4}$$

The composite trapezoidal formula corresponding to (4) is given by

$$\begin{aligned}I_{N_{x_1},N_{x_2}}Z((x_1)_j,(x_2)_i) = \frac{h_{x_1}h_{x_2}}{4}\sum_{p=0}^{i-1}\sum_{k=0}^{j-1}\Big[&\mathscr{K}((x_1)_j,(x_2)_i,(x_1)_k,(x_2)_p)Z((x_1)_k,(x_2)_p)\\ &+\mathscr{K}((x_1)_j,(x_2)_i,(x_1)_{k+1},(x_2)_p)Z((x_1)_{k+1},(x_2)_p)\\ &+\mathscr{K}((x_1)_j,(x_2)_i,(x_1)_k,(x_2)_{p+1})Z((x_1)_k,(x_2)_{p+1})\\ &+\mathscr{K}((x_1)_j,(x_2)_i,(x_1)_{k+1},(x_2)_{p+1})Z((x_1)_{k+1},(x_2)_{p+1})\Big].\end{aligned} \tag{5}$$

The remainder (truncation error) associated with the composite trapezoidal approximation is defined by $\tau^i_j = \left(I_{x_1,x_2}-I_{N_{x_1},N_{x_2}}\right)Z\left((x_1)_j,(x_2)_i\right)$, which represents the error incurred when approximating the double integral operator I_{x_1,x_2} by its discrete counterpart $I_{N_{x_1},N_{x_2}}$ at the grid point $\left((x_1)_j,(x_2)_i\right)$.
Using (3) and (5), problem (1) is transformed as

$$\begin{cases}\mathscr{D}^{\sigma}_{N_{x_1}}Z((x_1)_j,(x_2)_i)+A((x_1)_j,(x_2)_i)Z((x_1)_j,(x_2)_i)+\lambda I_{N_{x_1},N_{x_2}}Z((x_1)_j,(x_2)_i) = g((x_1)_j,(x_2)_i)+r^i_j,\\ Z(z_{1,0},(x_2)_i)=\phi((x_2)_i),\end{cases} \tag{6}$$

for $j=1,2,\ldots,N_{x_1}$, and $i=0,1,\ldots,N_{x_2}$. The remainder term r^i_j is given by $r^i_j=\varepsilon^i_j+\tau^i_j$. Neglecting r^i_j, the transformed problem (6) yields

$$\begin{cases}\dfrac{h_{x_1}^{-\sigma}}{\Gamma(2-\sigma)}\displaystyle\sum_{k=0}^{j-1}(Z^i_{k+1}-Z^i_k)d_{j-k}+A^i_jZ^i_j+\frac{\mu h_{x_1}h_{x_2}}{4}\sum_{p=0}^{i-1}\sum_{k=0}^{j-1}\Big\{\mathscr{K}((x_1)_j,(x_2)_i,(x_1)_k,(x_2)_p)Z^p_k\\ \quad+\mathscr{K}((x_1)_j,(x_2)_i,(x_1)_{k+1},(x_2)_p)Z^p_{k+1}+\mathscr{K}((x_1)_j,(x_2)_i,(x_1)_k,(x_2)_{p+1})Z^{p+1}_k\\ \quad+\mathscr{K}((x_1)_j,(x_2)_i,(x_1)_{k+1},(x_2)_{p+1})Z^{p+1}_{k+1}\Big\}=g^i_j,\\ Z^i_0=\phi_i,\end{cases} \tag{7}$$

for $j = 1,2,\ldots,N_{x_1}$ and $i = 0,1,\ldots,N_{x_2}$. Let $A^i_j = A((x_1)_j,(x_2)_i)$, and a similar notation is adopted for $g(x_1,x_2)$. The solution to the above numerical scheme can be explicitly represented as

$$\begin{cases} \Big\{\hat{b}_1 + A^i_j + \dfrac{\mu h_{x_1} h_{x_2}}{4}\mathscr{K}((x_1)_j,(x_2)_i,(x_1)_j,(x_2)_i)\Big\}Z^i_j = g^i_j + \hat{b}_1 Z^i_{j-1} + \displaystyle\sum_{k=0}^{j-2}(Z^i_k - Z^i_{k+1})\hat{b}_{j-k} \\ -\dfrac{\mu h_{x_1} h_{x_2}}{4}\displaystyle\sum_{p=0}^{i-1}\sum_{k=0}^{j-1}\Big\{\mathscr{K}((x_1)_j,(x_2)_i,(x_1)_k,(x_2)_p)Z^p_k + \mathscr{K}((x_1)_j,(x_2)_i,(x_1)_{k+1},(x_2)_p)Z^p_{k+1} \\ +\mathscr{K}((x_1)_j,(x_2)_i,(x_1)_k,(x_2)_{p+1})Z^{p+1}_k + \mathscr{K}((x_1)_j,(x_2)_i,(x_1)_{k+1},(x_2)_{p+1})Z^{p+1}_{k+1}\Big\}, \\ Z^i_0 = \phi_i, \end{cases} \tag{8}$$

for $i = 0,1,\ldots,N_{x_2}$ for each $j = 1,2,\ldots,N_{x_1}$, where $\hat{b}_p = \dfrac{d_p h_{x_1}^{-\sigma}}{\Gamma(2-\sigma)}$ for $p = 1,2,\ldots,N_{x_1}$.

Note. The discrete system (8) constitutes a linear algebraic system at each grid point (i,j). Hence, for a fixed time level j, the solution Z^j_i can be computed sequentially for all i. From a computational perspective, the presence of fractional and integral terms leads to nested summations, and therefore the overall computational cost increases with the number of grid points.

4 Numerical analysis

Lemma 1. *If $Z(x_1,x_2) \in \mathscr{C}^2([0,1]\times[0,1])$, is the solution of (1), then $|\varepsilon^i_j| \le C h^{2-\sigma}_{x_1}$, $j = 1,2,\ldots,N_{x_1}$.*

Proof. We have

$$\begin{aligned} |\varepsilon^i_j| &= \left|(\mathscr{D}^\sigma_{x_1} - \mathscr{D}^\sigma_{N_{x_1}})Z((x_1)_j,(x_2)_i)\right| \\ &= \left|\frac{1}{\Gamma(1-\sigma)}\sum_{k=0}^{j-1}\int_{(x_1)_k}^{(x_1)_{k+1}}\left[\frac{\partial Z}{\partial s}(s,(x_2)_i) - \frac{Z((x_1)_{k+1},(x_2)_i) - Z((x_1)_k,(x_2)_i)}{h_{x_1}}\right]\frac{ds}{((x_1)_j - s)^\sigma}\right| \\ &\le C\left|\frac{1}{\Gamma(1-\sigma)}\sum_{k=0}^{j-1}\int_{(x_1)_k}^{(x_1)_{k+1}}\frac{(x_1)_j + (x_1)_{j-1} - 2s}{((x_1)_j - s)^\sigma}ds + O(h^2_{x_1})\right|. \end{aligned}$$

From [8], we get

$$\left|\frac{1}{\Gamma(1-\sigma)}\sum_{k=0}^{j-1}\int_{(x_1)_k}^{(x_1)_{k+1}}\frac{(x_1)_j + (x_1)_{j-1} - 2s}{((x_1)_j - s)^\sigma}ds\right| \le 2h^{2-\sigma}_{x_1}.$$

Therefore, $|\varepsilon^i_j| \le C h^{2-\sigma}_{x_1}$. Hence complete the proof. □

Lemma 2. *Suppose $Z(x_1,x_2) \in \mathscr{C}^2([0,1]\times[0,1])$, then the remainder (5) satisfies*

$$|r^i_j| \le C(h^2_{x_1} + h^2_{x_2}) \quad \text{for} \quad j = 1,2,\ldots,N_{x_1};\ i = 1,2,\ldots,N_{x_2}.$$

Proof. By applying the Taylor series expansion, we obtain

$$
\begin{aligned}
|\tau_j^i| &= \left|(I_{x_1,x_2} - I_{N_{x_1},N_{x_2}})Z((x_1)_j,(x_2)_i)\right| \\
&= \Bigg|\sum_{p=0}^{i-1}\sum_{k=0}^{j-1}\int_{(x_2)_p}^{(x_2)_{p+1}}\int_{(x_1)_k}^{(x_1)_{k+1}}\frac{1}{2}\Big[(r-(x_1)_{k+\frac{1}{2}})^2\psi_{rr}(\zeta_r,\zeta_s)+(s-(x_2)_{p+\frac{1}{2}})^2\psi_{ss}(\eta_r,\eta_s) \\
&\quad +2(r-(x_1)_{k+\frac{1}{2}})(s-(x_2)_{p+\frac{1}{2}})\psi_{rs}(\tau_r,\tau_s)\Big]drds\Bigg|,
\end{aligned}
$$

where $\psi(x_1,x_2) = \mathscr{K}((x_1)_j,(x_2)_i,x_1,x_2)Z(x_1,x_2) \in \mathscr{C}^2([0,1]\times[0,1])$. Given that $\mathscr{K}$ is a smooth and $Z \in \mathscr{C}^2$, it follows that there exists a constant L which bounds all 2nd-order partial derivatives of ψ by L. We define the midpoints as $(x_1)_{k+\frac{1}{2}} = \frac{1}{2}((x_1)_k + (x_1)_{k+1})$ and $(x_2)_{p+\frac{1}{2}} = \frac{1}{2}((x_2)_p + (x_2)_{p+1})$. Applying triangle inequality, we obtain

$$
\begin{aligned}
|r_j^i| &\le \sum_{p=0}^{i-1}\sum_{k=0}^{j-1}\int_{(x_2)_p}^{(x_2)_{p+1}}\int_{(x_1)_k}^{(x_1)_{k+1}}\frac{1}{2}\Big[(r-(x_1)_{k+\frac{1}{2}})^2\left|\psi_{rr}(\zeta_r,\zeta_s)\right|+(s-(x_2)_{p+\frac{1}{2}})^2\left|\psi_{ss}(\eta_r,\eta_s)\right| \\
&\quad +2(r-(x_1)_{k+\frac{1}{2}})(s-(x_2)_{p+\frac{1}{2}})\left|\psi_{rs}(\tau_r,\tau_s)\right|\Big]drds \\
&\le \frac{L}{2}\sum_{p=0}^{i-1}\sum_{k=0}^{j-1}\Bigg[((x_2)_{p+1}-(x_2)_p)\int_{(x_1)_k}^{(x_1)_{k+1}}(r-(x_1)_{k+\frac{1}{2}})^2dr+((x_1)_{k+1}-(x_1)_k)\int_{(x_2)_p}^{(x_2)_{p+1}}(s-(x_2)_{p+\frac{1}{2}})^2ds \\
&\quad +2\int_{(x_2)_p}^{(x_2)_{p+1}}\int_{(x_1)_k}^{(x_1)_{k+1}}(r-(x_1)_{k+\frac{1}{2}})(s-(x_2)_{p+\frac{1}{2}})drds\Bigg] \\
&= \frac{L}{6}\sum_{p=0}^{i-1}\sum_{k=0}^{j-1}\left[h_{x_2}\frac{h_{x_1}^3}{4}+h_{x_1}\frac{h_{x_2}^3}{4}\right] \le \frac{L}{24}(h_{x_2}h_{x_1}^3+h_{x_1}h_{x_2}^3)N_{x_1}N_{x_2} \le C(h_{x_1}^2+h_{x_2}^2).
\end{aligned}
$$

□

Note: From Lemma 1, the truncation error of the $L1$ approximation is of order $O(h_{x_1}^{2-\sigma})$, while from Lemma 2, the quadrature error of the mixed integral term is of $O(h_{x_1}^2+h_{x_2}^2)$. Combining these estimates, the total local truncation error satisfies $|r_j^i| \le C\left(h_{x_1}^{2-\sigma}+h_{x_1}^2+h_{x_2}^2\right)$. Since $2-\sigma<2$, the dominant term is $O(h_{x_1}^{2-\sigma})$, leading to the overall convergence estimate.

Lemma 3. *For any mesh function $\{Z_j^i\}_{j=0}^{N_{x_1}}$ with $Z_0^i = 0$, we have*

$$
|Z_j^i| \le \max_{k=1,2,\ldots,j}\left\{\frac{h_{x_1}^\sigma\Gamma(2-\sigma)}{d_k}\mathscr{D}_{N_{x_1}}^\sigma|Z_k^i|\right\} \quad \text{for } j=1,2,\ldots,N_{x_1}.
$$

Proof. Suppose $\max\limits_{k=1,2,\ldots,j}|Z_k^i| = |Z_m^i|$ for some $m \in \{1,2,\cdots,j\}$. Since $Z_0^i = 0$, by using (3) without remainder term, we get

$$
\mathscr{D}_{N_{x_1}}^\sigma|Z_m^i| = \frac{h_{x_1}^{-\sigma}}{\Gamma(2-\sigma)}\left[|Z_m^i| - \sum_{k=1}^{m-1}(d_k-d_{k+1})|Z_{m-k}^i|\right].
$$

Now, since $d_1 = 1$ and $d_k > d_{k+1}$ for all $k \geq 1$, it follows that

$$\mathscr{D}^{\sigma}_{N_{x_1}}|Z^i_m| \geq \frac{h^{-\sigma}_{x_1}}{\Gamma(2-\sigma)}\left[|Z^i_m| - \sum_{k=1}^{m-1}\left(d_k - d_{k+1}\right)|Z^i_m|\right] \geq \frac{h^{-\sigma}_{x_1}}{\Gamma(2-\sigma)} d_m |Z^i_m|.$$

Therefore, $|Z^i_m| \leq \dfrac{h^{\sigma}_{x_1}\Gamma(2-\sigma)}{d_m}\mathscr{D}^{\sigma}_{N_{x_1}}|Z^i_m|$. □

Denote the absolute error by $\theta^i_j = Z((x_1)_j,(x_2)_i) - Z^i_j$ at $((x_1)_j,(x_2)_i)$, $j = 1,2,\ldots,N_{x_1}$; $i = 1,2,\ldots,N_{x_2}$. From (1) and (6), we obtain

$$\begin{cases} \mathscr{D}^{\sigma}_{N_{x_1}}\theta^i_j + A^i_j\theta^i_j + \lambda I_{N_{x_1},N_{x_2}}\theta^i_j = r^i_j, \\ \theta^i_0 = 0, \end{cases} \tag{9}$$

for $j = 1,2,\ldots,N_{x_1}$; $i = 1,2,\ldots,N_{x_2}$.

Theorem 2. *Suppose* $\Theta^{(i)} = (\theta^i_0,\theta^i_1,\ldots,\theta^i_{N_{x_1}})^T$ *and* $\Upsilon^{(i)} = (r^i_0,r^i_1,\ldots,r^i_{N_{x_1}})^T$. *Then, the solution of (9) satisfies the inequality*

$$\|\Theta^{(i)}\|_{\infty} \leq C\|\Upsilon^{(i)}\|_{\infty}.$$

Proof. Multiplying equation (9) by θ^i_j and applying equation (3), we obtain

$$\begin{aligned} &|\theta^i_j|^2 + \zeta|\theta^i_j|^2 + \frac{\mu h_{x_1}h_{x_2}}{4}\sum_{p=0}^{i-1}\sum_{k=0}^{j-1}\Big\{\mathscr{K}((x_1)_j,(x_2)_i,(x_1)_k,(x_2)_p)|\theta^p_k||\theta^i_j| \\ &+\mathscr{K}((x_1)_j,(x_2)_i,(x_1)_{k+1},(x_2)_p)|\theta^p_{k+1}||\theta^i_j| + \mathscr{K}((x_1)_j,(x_2)_i,(x_1)_k,(x_2)_{p+1})|\theta^{p+1}_k||\theta^i_j| \\ &+\mathscr{K}((x_1)_j,(x_2)_i,(x_1)_{k+1},(x_2)_{p+1})|\theta^{p+1}_{k+1}||\theta^i_j|\Big\} \leq |\Upsilon^{(i)}_j||\theta^i_j| + \sum_{k=1}^{j-1}\left(d_k - d_{k+1}\right)|\theta^i_{j-k}||\theta^i_j|. \end{aligned}$$

Since $\mathscr{K} > 0$, one has

$$|\theta^i_j|^2 \leq |\Upsilon^{(i)}_j||\theta^i_j| + \sum_{k=1}^{j-1}\left(d_k - d_{k+1}\right)|\theta^i_{j-k}||\theta^i_j|.$$

Upon division by $|\theta^i_j|$, the inequality takes the form

$$\mathscr{D}^{\sigma}_{N_{x_1}}|\theta^i_j| \leq |\Upsilon^{(i)}_j|.$$

Since $d_1 = 1$ and $d_q > d_{q+1}$, $q \geq 1$, it follows that

$$(1-\sigma)q^{-\sigma} \leq d_q \leq (1-\sigma)(q-1)^{-\sigma} \quad \text{for} \quad q \geq 2.$$

Applying Lemma 3, we deduce

$$\begin{aligned} |\theta^i_j| &\leq \max_{k=1,2,\ldots,j}\left\{\frac{h^{\sigma}_{x_1}\Gamma(2-\sigma)}{d_k}|\Upsilon^{(i)}_k|\right\} \\ &\leq \frac{h^{\sigma}_{x_1}\Gamma(2-\sigma)}{(1-\sigma)N^{-\sigma}_{x_1}}\max_{k=1,2,\ldots,j}\left\{|\Upsilon^{(i)}_k|\right\} \leq C\max_{k=1,2,\ldots,j}\left\{|\Upsilon^{(i)}_k|\right\}. \end{aligned}$$

□

Theorem 3. *Let $Z((x_1)_j,(x_2)_i)$ be the exact solution, and Z_j^i the corresponding numerical approximation to problem (1), then the following holds*

$$\|Z((x_1)_j,(x_2)_i)-Z_j^i\|_\infty \leq C\left(h_{x_1}^{2-\sigma}+h_{x_2}^2\right),$$

for $j=1,2,\ldots,N_{x_1}$, $i=1,2,\ldots,N_{x_2}$.

Proof. Lemma 1 and Lemma 2 show that

$$|\Upsilon_j^{(i)}| \leq |\varepsilon_j^i|+|\Upsilon_j^i| \leq C\left(h_{x_1}^{2-\sigma}+h_{x_1}^2+h_{x_2}^2\right).$$

Using Theorem 2, we obtain

$$\|\Theta^{(i)}\|_\infty \leq \Gamma(1-\sigma)\|\Upsilon^{(i)}\|_\infty \leq C\Gamma(1-\sigma)\left(h_{x_1}^{2-\sigma}+h_{x_1}^2+h_{x_2}^2\right) \leq C\left(h_{x_1}^{2-\sigma}+h_{x_2}^2\right).$$

This proves the theorem. □

5 Numerical illustrations

The proposed scheme has been validated through the following two numerical examples. We evaluate the maximum error as $\Sigma_{N_{x_1}}^{N_{x_2}} = \max\limits_{0\leq j\leq N_{x_1}} \max\limits_{0\leq i\leq N_{x_2}} \left|Z((x_1)_j,(x_2)_i)-Z_j^i\right|$, and the the order of convergence as $\rho_{N_{x_1}}^{N_{x_2}} = \log_2\left(\Sigma_{N_{x_1}}^{N_{x_2}}/\Sigma_{2N_{x_1}}^{2N_{x_2}}\right)$.

Example 1. Consider the test case

$$\begin{cases} \mathscr{D}_{x_1}^{\sigma} Z + \displaystyle\int_0^{x_2}\int_0^{x_1} (x_2+s)Z(r,s)drds = \frac{2x_1^{2-\sigma}x_2}{\Gamma(3-\sigma)} + \frac{5x_1^3x_2^3}{18} \quad \text{for } (x_1,x_2)\in(0,1]\times[0,1], \\ Z(0,x_2)=0. \end{cases}$$

The exact solution is given by $Z(x_1,x_2)=x_1^2x_2$. Figure 1 presents both the exact and numerical solutions for $\sigma=0.3$ corresponding to Example 1. The comparison illustrated in Figure 2 presents the exact and approximate solutions across different values of x_1 and x_2, with $\sigma=0.7$. The surface plot in Figure 3(a) and the log-log error plot in Figure 3(b) demonstrate that the implemented technique attains a sharp rate of convergence. Table 1 lists the values of $\Sigma_{N_{x_1}}^{N_{x_2}}$ and $\rho_{N_{x_1}}^{N_{x_2}}$ for Example 1.

Example 2. Consider the test case

$$\begin{cases} \mathscr{D}_{x_1}^{\sigma} Z + (1-x_1x_2)Z - \displaystyle\int_0^{x_2}\int_0^{x_1} (x_1\cos(r)+x_2s)Z(r,s)drds = g(x_1,x_2), \\ Z(0,x_2)=\sin(x_2). \end{cases}$$

Choose the function $g(x_1,x_2)$ so that the exact solution is $Z(x_1,x_2)=e^{x_1}\sin(x_2)$. Figure 4 displays the exact and computed solutions with $\sigma=0.3$ for Example 2, while Figure 5 illustrates a comparison between the exact and computed solutions for different x_1 and x_2 with $\sigma=0.7$. For a uniform mesh, Figure 6(a) shows the surface plot of the computational error for Example 2. Log-log plot in Figure 6(b), and $\Sigma_{N_{x_1}}^{N_{x_2}}, \rho_{N_{x_1}}^{N_{x_2}}$ are displayed in Table 2, illustrating that the convergence rate is sharp. The computed solution is found to be convergent with the exact solution based on experimental data.

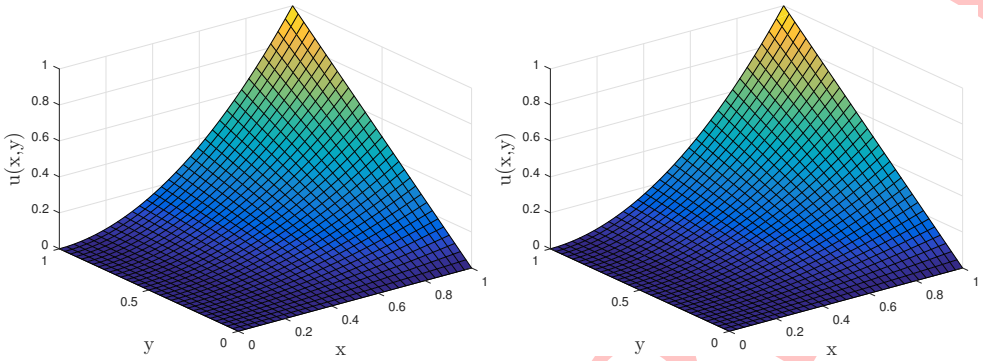

(a) Exact **(b)** Numerical

Figure 1: Computed solution with $\sigma = 0.3$ and $N_{x_1} = N_{x_2} = 32$ for Example 1

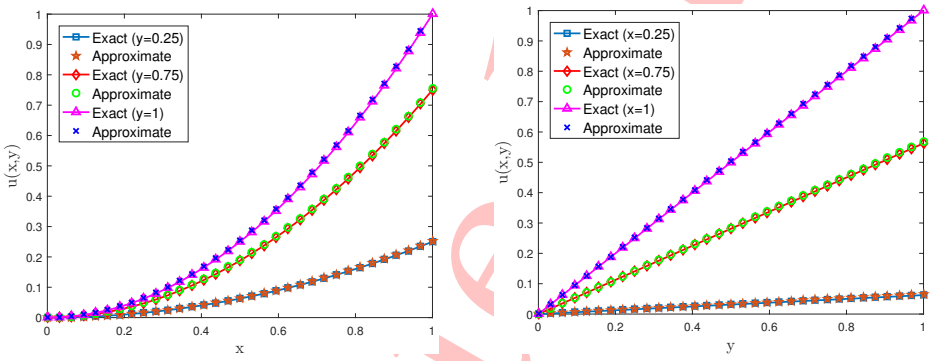

(a) **(b)**

Figure 2: Exact versus computed solutions with $\sigma = 0.7, N_{x_1} = N_{x_2} = 32$ for Example 1

Table 1: $\Sigma_{N_{x_1}}^{N_{x_2}}$, $\rho_{N_{x_1}}^{N_{x_2}}$ *and CPU time (in second) with* $N_{x_1} = N_{x_2}$ *for Example 1*

$\sigma \downarrow$	8	16	32	64	128	Time(s)
0.1	1.514E-03	3.498E-04	7.944E-05	2.107E-05	6.378E-06	1.51E+01
	2.114	2.139	1.915	1.724	–	
0.2	1.894E-03	6.537E-04	2.127E-04	6.721E-05	2.083E-05	1.41E+01
	1.535	1.620	1.662	1.690	–	
0.4	7.413E-03	2.691E-03	9.453E-04	3.258E-04	1.109E-04	1.42E+01
	1.462	1.509	1.537	1.555	–	
0.6	2.065E-02	8.325E-03	3.269E-03	1.265E-03	4.857E-04	1.41E+01
	1.311	1.349	1.369	1.381	–	
0.8	4.935E-02	2.239E-02	9.958E-03	4.384E-03	1.920E-03	1.40E+01
	1.140	1.169	1.184	1.191	–	
0.9	7.227E-02	3.484E-02	1.652E-02	7.772E-03	3.642E-03	1.40E+01
	1.053	1.076	1.088	1.094	–	

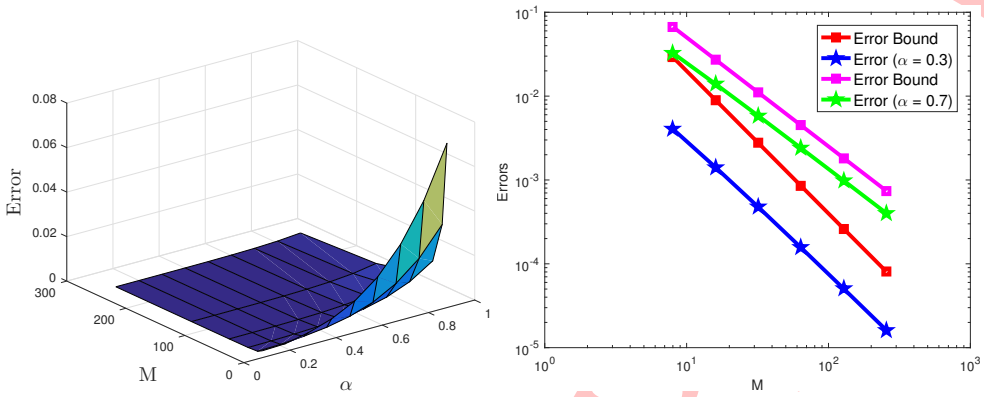

(a) **(b)**

Figure 3: Surface plot and log-log plot of $\Sigma_{N_{x_1}}^{N_{x_2}}$ for Example 1

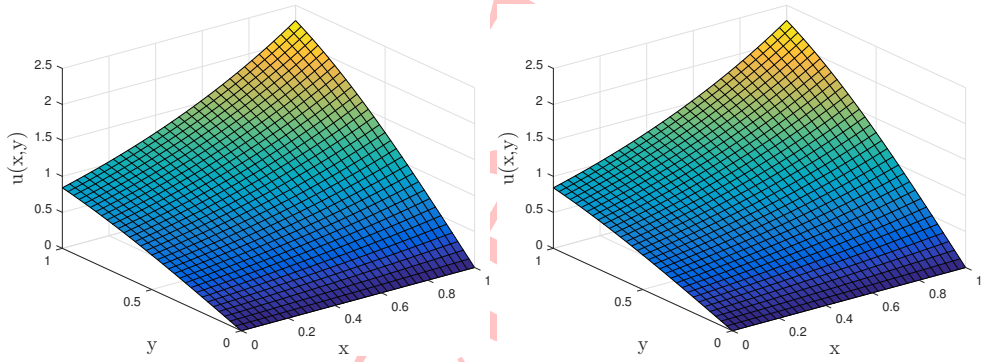

(a) Exact **(b)** Numerical

Figure 4: Computed solution with $\sigma = 0.3$ and $N_{x_1} = N_{x_2} = 32$ for Example 2

Table 2: $\Sigma_{N_{x_1}}^{N_{x_2}}$, $\rho_{N_{x_1}}^{N_{x_2}}$ *and CPU time (in second) with* $N_{x_1} = N_{x_2}$ *for Example 2*

$\sigma \downarrow$	8	16	32	64	128	Time(s)
0.1	3.988E-03	1.098E-03	3.018E-04	8.282E-05	6.195E-06	1.85E+01
	1.861	1.862	1.866	1.869	–	
0.3	9.398E-03	2.985E-03	9.436E-04	2.966E-04	2.895E-05	1.81E+01
	1.654	1.662	1.669	1.676	–	
0.5	1.926E-02	6.948E-03	2.498E-03	8.945E-04	1.135E-04	1.79E+01
	1.471	1.476	1.482	1.487	–	
0.7	3.692E-02	1.507E-02	6.163E-03	2.517E-03	4.178E-04	1.80E+01
	1.293	1.290	1.292	1.294	–	
0.9	6.814E-02	3.132E-02	1.453E-02	6.769E-03	1.473E-03	1.81E+01
	1.121	1.108	1.102	1.101	–	

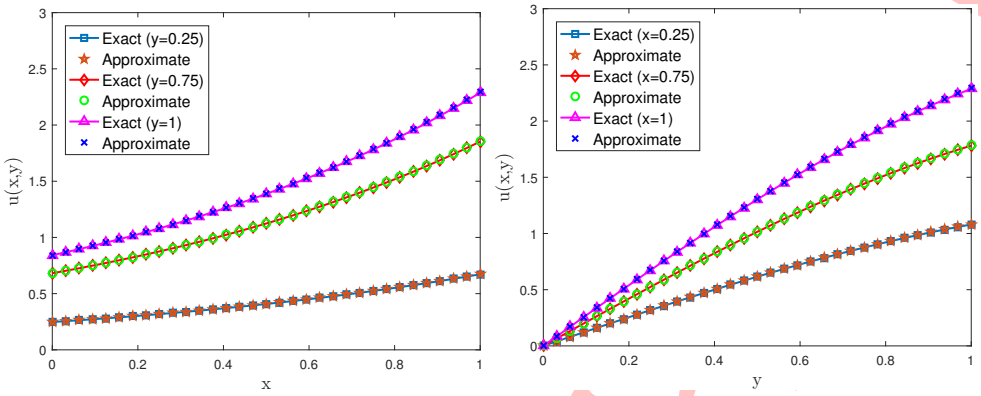

(a) **(b)**

Figure 5: Exact versus computed solutions for Example 2 with $\sigma = 0.7$ and $N_{x_1} = N_{x_2} = 32$

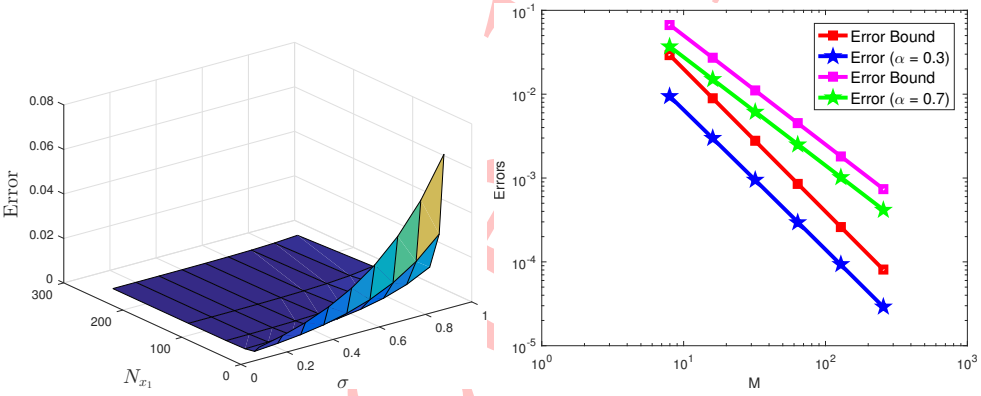

(a) **(b)**

Figure 6: Surface plot and log-log plot of $\Sigma_{N_{x_1}}^{N_{x_2}}$ for Example 2

Example 3. Consider the test case

$$\begin{cases} \mathscr{D}_{x_1}^{\sigma} Z + (x_1+x_2)^2 Z + \displaystyle\int_0^{x_2}\int_0^{x_1} Z(r,s)drds = g(x_1,x_2) \ \text{ for } \ (x_1,x_2) \in (0,1]\times[0,1], \\ Z(0,x_2) = e^{x_2}. \end{cases}$$

Choose the function $g(x_1,x_2)$ so that the exact solution is $Z(x_1,x_2) = e^{x_1+x_2}$. The maximum error $\Sigma_{N_{x_1}}^{N_{x_2}}$ and the corresponding rate of convergence $\rho_{N_{x_1}}^{N_{x_2}}$, along with the CPU time required for each computation, are presented in Table 3. The results clearly demonstrate that the proposed scheme achieves the expected convergence rate, confirming the sharpness of the theoretical estimate. Moreover, the reported CPU time indicates that the method remains computationally efficient for the considered mesh sizes. Overall, the numerical results show that the computed solution converges to the exact solution, thereby validating the accuracy and effectiveness of the proposed numerical approach.

Table 3: *Maximum pointwise error, order of convergence, and CPU time (in seconds) for Example 3*

$\alpha\downarrow$	8	16	32	64	128	Time(s)
0.2	3.083E-03	7.392E-04	2.359E-04	7.306E-05	2.222E-05	1.49E+01
	2.060	1.648	1.691	1.717	–	
0.4	7.564E-03	2.755E-03	9.661E-04	3.317E-04	1.125E-04	1.42E+01
	1.457	1.512	1.542	1.560	–	
0.6	1.906E-02	7.704E-03	3.027E-03	1.172E-03	4.499E-04	1.42E+01
	1.307	1.347	1.369	1.381	–	
0.8	4.196E-02	1.904E-02	8.490E-03	3.747E-03	1.643E-03	1.42E+01
	1.140	1.165	1.180	1.189	–	
0.9	7.514E-02	3.787E-02	1.869E-02	9.123E-03	4.430E-03	1.42E+01
	0.989	1.019	1.034	1.042	–	

Example 4. Consider the test case

$$\begin{cases} \mathscr{D}^{\sigma}_{x_1} Z + \displaystyle\int_0^{x_2}\int_0^{x_1} (x_1^2 r + x_2^2 s) Z(r,s)\,dr\,ds = x_1^3 \ \text{ for } \ (x_1,x_2) \in (0,1]\times[0,1], \\ Z(0,x_2) = e^{x_2}. \end{cases}$$

In this example, the exact solution is not available in closed form, and hence a direct computation of the numerical error is not possible. To address this, we employ the double mesh principle, which is a commonly used technique for error estimation in such situations. In this approach, the numerical solution obtained on a sufficiently refined mesh is treated as a reference solution. The solution computed on a coarser mesh is then compared with this reference solution, and the maximum difference between them is taken as an estimate of the error. This procedure enables us to assess the convergence behavior and accuracy of the proposed numerical scheme even in the absence of an exact solution. The results obtained in Table 4 demonstrate that the method exhibits stable and consistent convergence, thereby confirming its effectiveness.

Table 4: *Maximum pointwise error, order of convergence, and CPU time (in seconds) for Example 4*

$\alpha\downarrow$	8	16	32	64	128	Time(s)
0.3	7.683E-03	2.646E-03	9.287E-04	3.110E-04	1.014E-04	2.36E+02
	1.538	1.511	1.578	1.616	–	
0.5	1.345E-02	5.566E-03	2.153E-03	8.038E-04	2.940E-04	2.36E+02
	1.273	1.370	1.422	1.451	–	
0.7	2.124E-02	9.354E-03	3.991E-03	1.673E-03	6.931E-04	2.37E+02
	1.183	1.229	1.254	1.272		
0.9	2.911E-02	1.378E-02	6.487E-03	3.047E-03	1.428E-03	2.37E+02
	1.079	1.086	1.090	1.093	–	

6 Conclusion

The current study presents an effective difference scheme for addressing fractional Volterra integro-differential equations involving mixed integral terms. The fractional operator is discretized using the standard $L1$ technique, while the mixed integral component is approximated using the composite trapezoidal rule. A detailed convergence and error analysis is presented, demonstrating that the numerical scheme attains an accuracy of order $(2-\sigma)$. Both theoretical results and numerical illustrations validate the efficacy and reliability of the implemented scheme.
Future work may focus on improving the accuracy of the method by employing nonuniform meshes, particularly to better capture the singular behaviour near the origin. In addition, the extension of the proposed approach to problems involving singular kernels, as well as its application to irregular domains and higher-dimensional problems, constitutes an interesting and promising direction for further research.

Conflict of interest

The authors declare that there are no conflicts of interest.

References

[1] S. Ahsan, R. Nawaz, M. Akbar, K.S. Nisar, K.M. Abualnaja, E.E. Mahmoud, A H. Abdel-Aty, *Numerical solution of two-dimensional fractional order Volterra integro-differential equations*, AIP Advances **11(3)** (2021) 035232.

[2] N. Bellomo, B. Firmani, L. Guerri, *Bifurcation analysis for a nonlinear system of integro-differential equations modelling tumor-immune cells competition*, Appl. Math. Lett. **12** (1999) 39-–44.

[3] A. Boutiara, *A novel implementation of fixed-point theorems for high-order Hadamard fractional differential equations with multi-point integral boundary conditions*, J. Math. Model. **11(4)** (2023) 767–782.

[4] H. Dehestani, Y. Ordokhani, *Developing the discretization method for fractal-fractional two-dimensional Fredholm–Volterra integro-differential equations*, Math. Methods Appl. Sci. **44** (2021) 14256–14273.

[5] K. Diethelm, *The Analysis of Fractional Differential Equations: An Application-Oriented Exposition Using Differential Operators of Caputo Type*, Springer-Verlag, Berlin, 2010.

[6] B. Ghosh, J. Mohapatra, *Numerical solution for a system of time fractional Volterra integro-differential equations*, Miskolc Math. Notes **26** (2025) 395–410.

[7] J. He, *Some applications of nonlinear fractional differential equations and their approximations*, Bull. Sci. Technol. **15** (1999) 86–90.

[8] Y. Lin, C. Xu, *Finite difference/spectral approximations for the time-fractional diffusion equation*, J. Comput. Phys. **225** (2007) 1533–1552.

[9] J. Mohapatra, *Equidistribution grids for two-parameter convection–diffusion boundary-value problems*, J. Math. Model. **2(1)** (2014) 1–21.

[10] J. Mohapatra, S.P. Mohapatra, A. Nath, *An approximation technique for a system of time-fractional differential equations arising in population dynamics*, J. Math. Model. **13(3)** (2025) 519–531.

[11] M. Mojahedfar, A. Tari Marzabad, *Solving two-dimensional fractional integro-differential equations by Legendre wavelets*, Bull. Iran. Math. Soc. **43** (2017) 2419–2435.

[12] S. Nemati, P.M. Lima, Y. Ordokhani, *Numerical solution of a class of two-dimensional nonlinear Volterra integral equations using Legendre polynomials*, J. Comput. Appl. Math. **242** (2013) 53–69.

[13] A. Panda, B. Ghosh, J. Mohapatra, *Efficient numerical techniques for fractional integro-differential equations with weakly singular kernel*, Phys. Scr. **100** (2024) 015201.

[14] I. Podlubny, *Fractional Differential Equations*, Academic Press, San Diego, 1998.

[15] M.Y. Rahimi, S. Shahmorad, F. Talati, A. Tari, *An operational method for the numerical solution of two-dimensional linear Fredholm integral equations with an error estimation*, Bull. Iran. Math. Soc. **36(2)** (2010) 119—132.

[16] Y.A. Rossikhin, M.V. Shitikova, *Application of fractional calculus for dynamic problems of solid mechanics: novel trends and recent results*, Appl. Mech. Rev. **63(1)** (2010) 010801.

[17] A. Tari, S. Shahmorad, *A computational method for solving two-dimensional linear Fredholm integral equations of the second kind*, ANZIAM J. **49(4)** (2008) 543-–549.

[18] H. Wang, H.M. Fu, H.F. Zhang, *A practical thermodynamic method to calculate the best glass-forming composition for bulk metallic glasses*, Int. J. Nonlinear Sci. Numer. Simul. **8(2)** (2007) 171-–178.